

Droplet Manipulation With Light on Optoelectrowetting Device

Pei-Yu Chiou, *Member, IEEE*, Zehao Chang, and Ming C. Wu, *Fellow, IEEE*

Abstract—We have demonstrated a 2-D droplet manipulation platform allowing fully optical manipulation of droplets on a photosensitive surface. Optically controlled injection, transport, separation, and multiple droplet manipulation have been achieved for nanoliter-size droplets. These functions are realized by sandwiching the droplets between two optoelectrowetting (OEW) surfaces. Optical illumination on OEW surfaces changes the surface wettability locally through the electrowetting mechanism. Optical illumination turns the initially Teflon-coated surface from hydrophobic to hydrophilic. This process is reversible and can be controlled in real time. We have achieved a maximum transport speed of 78 mm/s for a 100-nL droplet using a scanning laser beam. We have also demonstrated a fully decoupled 2-D multidroplet manipulation on the OEW surfaces. Potentially, the OEW mechanism can be scaled up to process a large number of liquid droplets using projected optical images for high throughput applications. [2007-0054]

Index Terms—Electrowetting, laboratory-on-a-chip, optoelectrowetting (OEW), surface tension.

I. INTRODUCTION

MICROFLUIDIC devices offer many advantages in the fields of chemical and biological analysis [1], [2]. Droplet-based microfluidic devices have attracted much interest since they provide flexible and reconfigurable platforms for microfluidic processing [3]–[7]. Digitalized droplets containing different chemical or biological reagents can be transported and mixed to realize multistep diagnostic protocols on the same chip. Electrowetting on dielectric is an effective mechanism for manipulating droplets in microscale [8]–[10]. The surface tension between the solid and liquid interfaces can be modulated through the electrostatic energy that is stored in the insulation layer by lithographically patterned electrodes. Activating these electrodes can decrease the droplet contact angle and perform various droplet functions, including injection, separation, transport, and mixing [11], [12]. Several diagnostic microfluidic devices have also been successfully demonstrated [5], [13], [14].

To increase the throughput of testing, simultaneous control of a large number of droplets is required. Previously, most of the electrowetting devices used a linear array of elec-

trodes, limiting their capability to sequential processing. A 2-D array of electrodes is more versatile; however, individual addressing of electrodes requires complex wiring and integration of on-chip decoders as used in electronic memory chips. Fan *et al.* has proposed a driving algorithm using cross-reference electrodes and a time-multiplexed scheme to manipulate multiple droplets on a 2-D surface. This method has successfully reduced the wiring number from $N \times M$ to $N + M$ [15], [16]. However, the efficiency of this sequential scanning method decreases rapidly as the droplet number increases since the driving duration after the average over the total droplets becomes too short to actuate droplets and fast refreshing is challenging, which is similar to the limitation of using a passive electrode matrix to drive liquid-crystal displays. On-chip address decoders have been used to address a similar 2-D array of electrodes in dielectrophoretic devices [4], however, at the expense of the chip cost as the entire chip needs to be fabricated using complementary metal–oxide–semiconductor process.

Previously, we have proposed an optoelectrowetting (OEW) mechanism to simultaneously address a large number of electrowetting electrodes with light [17]. In OEW devices, thousands of electrodes are connected to a common bias through a photoconductive material. Upon illumination, the photoconductivity increases for several orders and turn on the illuminated electrode to trigger electrowetting effect. The OEW mechanism allows optical images to actuate electrowetting locally with desired area, shape, and position. By reconfiguring optical images, dynamic electrowetting allows transporting of droplets in real time.

In this paper, we report on the full set of droplet manipulation functions including droplet transport, generation, separation, and multidroplet manipulation on OEW devices using laser beams. The results have promised OEW to be a powerful mechanism in manipulating a large number of droplets on a 2-D surface.

II. DEVICE STRUCTURE AND FABRICATION

A schematic diagram of the OEW-based microfluidic system is shown in Fig. 1(a). Multiple droplets with different reagents, buffer solutions, or other compounds are injected from the reservoirs, thoroughly mixed, and transported to testing area. The droplet can be divided into smaller droplets for multiple testing.

The schematic structure of an OEW surface is shown in Fig. 1(b). It consists of multiple transparent layers, including a glass substrate, a 2000-Å indium–tin–oxide (ITO) layer,

Manuscript received March 6, 2007; revised June 2, 2007. This work was supported in part by the Defense Advanced Research Projects Agency Optoelectronics Center through the Center for Heterogeneously Integrated Photonics under Contract MDA972-00-1-0019. Subject Editor E. Obermeier.

P.-Y. Chiou and Z. Chang are with the University of California, Los Angeles, CA 90095 USA (e-mail: pychiou@seas.ucla.edu).

M. C. Wu is with the University of California, Berkeley, CA 94720 USA. Color versions of one or more of the figures in this paper are available online at <http://ieeexplore.ieee.org>.

Digital Object Identifier 10.1109/JMEMS.2007.904336

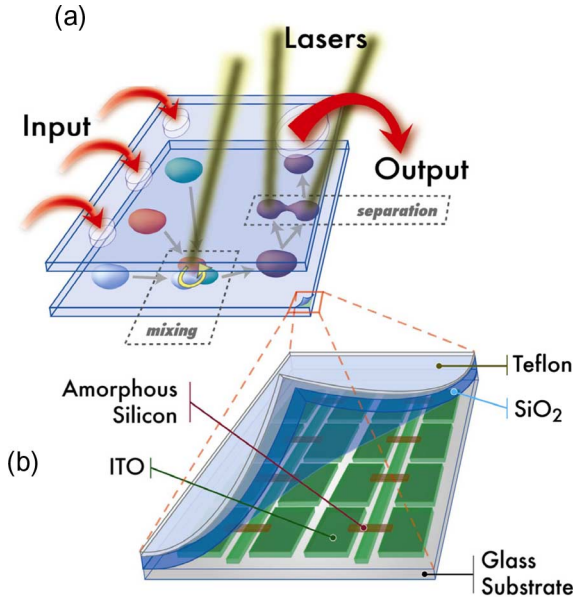


Fig. 1. (a) Schematic illustration of liquid droplet manipulation in an OEW device. (b) Schematic of the OEW device structure.

a 5000-Å silicon dioxide (SiO₂) layer that is deposited by plasma-enhanced chemical vapor deposition (PECVD). The device was then primed in hexamethyldisilazane vapor, spin coated (1500 r/min and 30 s) with 0.5% Teflon-AF (from DuPont), and baked on a hot plate (150 °C for 10 min to form a 500-Å hydrophobic Teflon layer. The electro-wetting electrodes and the biasing lines are patterned in the ITO layer and connected through undoped hydrogenated amorphous silicon (a-Si:H) strips that are deposited by PECVD and patterned by reactive ion etching. The a-Si:H is a photosensitive material that has been widely used in solar cell and flat-panel display industries. The undoped a-Si:H has high dark electrical resistivity and can effectively isolate the electrodes from the bias grid. Under light illumination, its photoconductivity increases for several orders of magnitude and to turn on the connected electrodes. A 10-nm-thick aluminum layer is deposited between the ITO and the undoped a-Si layer to lower the contact resistance.

Fig. 2(a) shows a fabricated transparent OEW device. The photosensitive region that is marked by dashed lines has an area of 1 cm × 1 cm. The microscopic pictures of the photoconductive electrode arrays are shown in Fig. 2(b). Each cell contains two ITO electrodes and an a-Si:H bridge connecting the electrodes to the bias line. The gap spacing between the bias line and the electrode is 5 μm, and the width of the bridge is 30 μm. Each electrode has a size of 50 μm × 100 μm.

III. OEW MECHANISM

Fig. 3(a) illustrates the operating principle of the OEW device. A liquid droplet is sandwiched between two OEW surfaces, and an ac voltage is applied across the structure. The ITO grids on the same OEW surface are connected together and have the same electrical potential. At the area without light illumination, the droplet has a contact angle of 105° due to the hydrophobic Teflon surface. The a-Si:H strip has an impedance

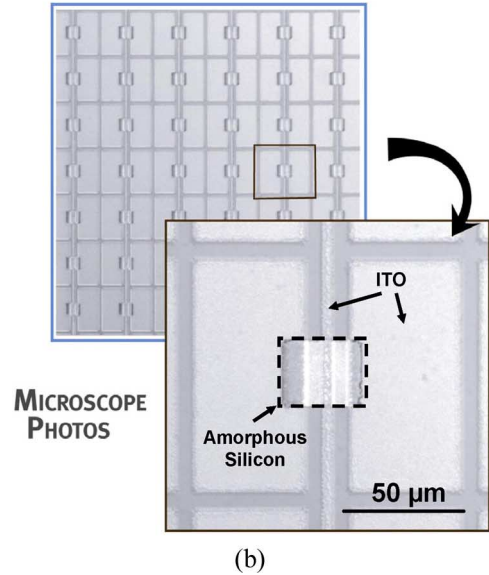
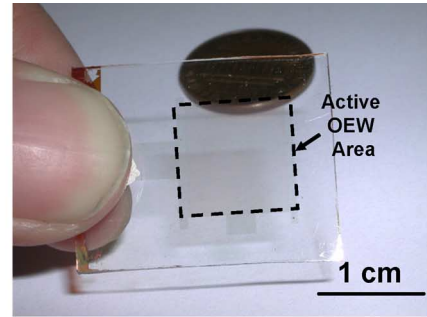


Fig. 2. (a) Fabricated OEW device (one side). The active OEW area is marked by the dashed-line square. (b) Microscopic pictures showing part of the (top) active OEW area and (bottom) structure of an OEW cell.

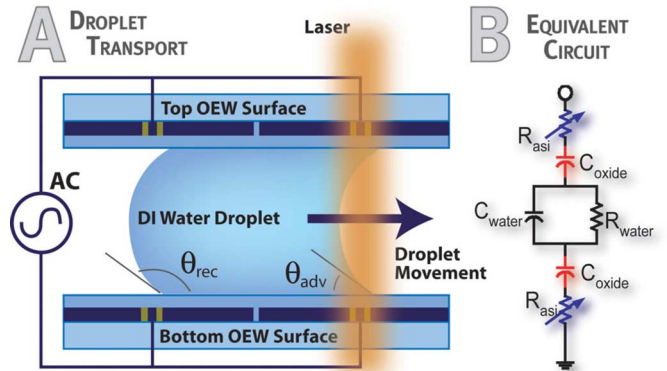


Fig. 3. (a) Illustration of contact angle change on OEW surface. (b) Equivalent circuit for one unit cell of the OEW device. R_{asi} is the resistance of the a-Si photoconductor under light illumination, C_{oxide} is the capacitance of the SiO₂ insulator, and C_{water} and R_{water} are the capacitance and resistance of water layer between the two OEW surfaces.

on the order of $10^{13} \Omega$ in the dark. Under an ac frequency of 500 Hz, it dominates over the $10^9 \Omega$ impedance of a capacitor between an ITO electrode and the liquid layer, resulting in a majority voltage drop across the a-Si bridge and a small contact angle change in the dark area. At the area with light illumination, the resistivity of the a-Si:H strip decreases to less

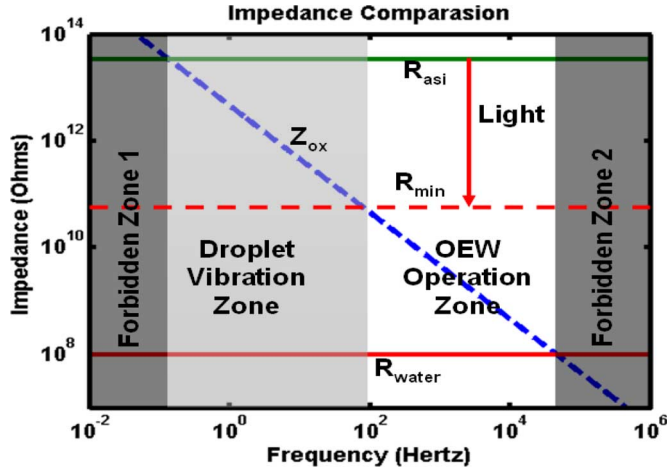


Fig. 4. Frequency response of the electrical impedance of the various components in an equivalent circuit model. OEW operation is divided into four different zones. The dashed line represents the reduced resistance of the a-Si strip under light illumination.

than $10^9 \Omega$, and the capacitor on the ITO electrode starts to get charged and induces the electrowetting effect. The illuminated surface becomes hydrophilic, and the droplet contact angle decreases to less than 90° . This creates an asymmetric droplet meniscus between the dark and illuminated sides of the droplet, and a net pressure resulting from surface tension forces moves the droplet toward the light beam. Steering the light beam can drag the illuminated droplets continuously on an OEW surface.

This optically induced electrowetting process can be better explained with an equivalent circuit model shown in Fig. 3(b). This circuit model includes the top and bottom OEW cells, and a liquid droplet in between. The a-Si strip is modeled as variable resistor R_{asi} , and the capacitor between the liquid and the ITO electrode is represented by C_{oxide} . The liquid droplet is a parallel combination of C_{water} and R_{water} . The term C_{water} is usually negligible compared to R_{water} , because we operate at an ac frequency that is much lower than the RC relaxation time of water. This simplifies the equivalent circuit model to a serial connection of two R_{asi} 's, two C_{oxide} 's, and one R_{water} . For OEW devices in this paper, these values are $3.3 \times 10^{13} \Omega$ (without light), $3.5 \times 10^{-13} \text{ F}$, and $10^8 \Omega$, respectively. The conductivity that is used for a-Si and DI water droplet is 10^{-10} and 10^{-6} S/cm , respectively.

Since the OEW mechanism relies on the switching of voltage drops between photoconductors and oxide capacitors, its operation is ac frequency dependent. Fig. 4 shows the frequency response of these impedances. The impedance of an oxide capacitor decreases monotonically due to its capacitive nature, but the impedance of the a-Si bridge and water is constant at ac frequencies where OEW operates. As shown in Fig. 4, there is a frequency window that OEW devices can operate. In the low-frequency range, the electrical impedance of C_{oxide} is larger than R_{asi} in the dark state, which means that the C_{oxide} term dominates and the electrowetting effect is activated everywhere on OEW surfaces even without optical illumination. No optical control is allowed. In high ac frequency, the impedance of C_{oxide} becomes smaller than R_{water} . Optical illumination will switch the voltage to the bulk water layer, instead of the capaci-

tor. No electrowetting effect will occur on OEW surfaces, even under strong light illumination. Optical actuation of droplets on OEW surfaces will only be achieved at an ac frequency within this window. In our experiments, we also observed that droplets vibrate when the ac frequency is smaller than 100 Hz. It is hard to control and confine the droplet with light in the vibration zone. The optimal OEW operation frequency is between 100 and 700 Hz, although the frequency window extends to 30 kHz, as shown in Fig. 4. Operating at high frequency in this window is allowed but requires a stronger light illumination. The dotted line represents the minimum impedance of an a-Si bridge under light illumination.

IV. EXPERIMENT RESULT AND DISCUSSION

A. Droplet Transport

Transporting a droplet can be achieved simply by trapping a droplet and scanning a light beam across the OEW surface. The trapped droplet will follow the trace of the moving beam. The size of the droplet under test is about 1 mm in diameter (this droplet is created by the droplet injection and separation process that will be discussed later in this section). A light beam with a spot size of 1 mm covers about 140 electrode cells simultaneously during droplet transportation. There is no need to align the top and bottom OEW electrodes since the light beam penetrates through both surfaces and self-aligns the active electrowetting area for droplet transport. Theoretically, the minimum droplet size that can be transported in this OEW device is about $100 \mu\text{m}$ in diameter, which is approximately the size of an electrode cell.

In our experiment, we use a 5-mW 532-nm laser beam with a spot size of 1 mm as the light source and a programmable galvanometer scanning mirrors (Cambridge Technology, model 6860) to steer the laser beam. Fig. 5 shows snapshots from the recorded video. It shows that the droplet can follow a scanning speed up to 78 mm/s.

B. Droplet Separation

Droplet separation is an important function for controlling droplet volume. To split a droplet, we use two light beams to illuminate the two opposite edges of a droplet, as illustrated in Fig. 6. Before illumination, the contact angle is larger than 90° in both cross sections along ab and cd. When light beams illuminate at the two opposite edges, the contact angle at these two edges decreases to less than 90° due to the electrowetting effect. The droplet is elongated along the cd cross section, as shown in Fig. 6(b). At the middle of the droplet, the contact angle remains to be larger than 90° along the ab cross section, because there is no light illumination in this area. This creates a force that narrows the middle neck of the droplet and breaks the droplet into two when the two laser beams move far enough, as shown in Fig. 6(c).

C. Droplet Injection

Injection is the process of generating a droplet from a liquid reservoir. The reservoir is defined by a large electrowetting area

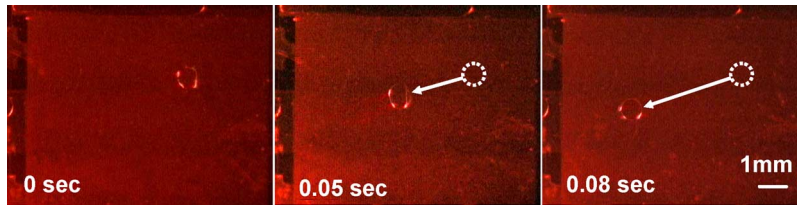


Fig. 5. Droplet transport by a scanning laser beam. The maximum measured moving speed is 78 mm/s by applying a 100-V ac voltage with a frequency of 500 Hz.

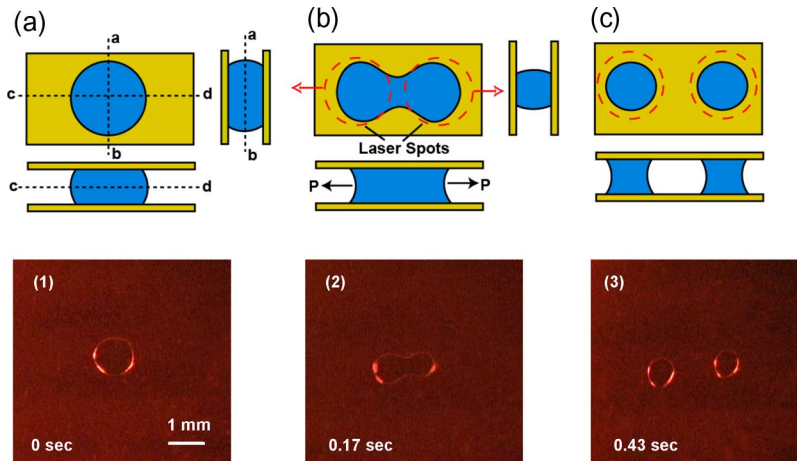


Fig. 6. Schematic drawing of the top view and two cross-sectional views (ab and cd) as well as the corresponding top-view micrographs of the droplet during separation process. (a) Before separation. (b) Two laser beams pulling the droplet along the cd direction. (c) Separation finishes.

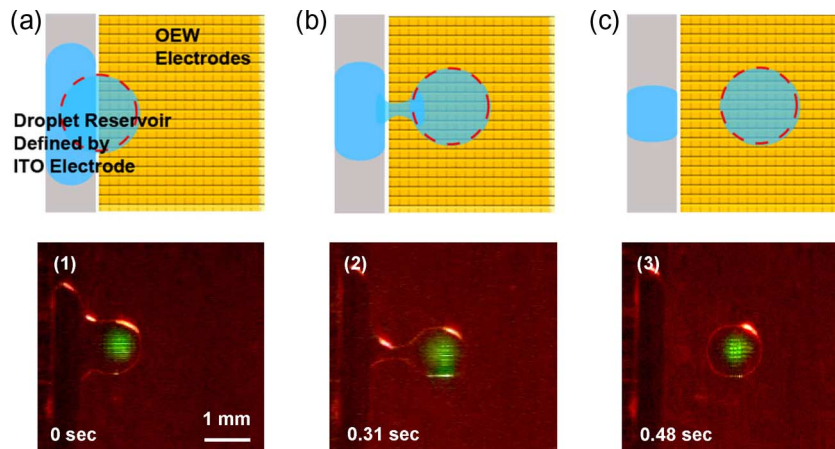


Fig. 7. Schematic diagrams and snapshots (top view) illustrating the droplet injection process. (a) Before injection. (b) In the middle of injection. (c) Injected droplet trapped by light beam.

that is patterned directly by the ITO electrodes. This process is very similar to droplet separation, except that only one laser beam is required, as shown in Fig. 7. As the light beam moves across the reservoir, a droplet with a size that is similar to the spot size of the light beam is dragged out from the reservoir into the active OEW region for later processing.

D. Multidroplet Manipulation

We have also demonstrated a fully decoupled multidroplet transport capability using multiple scanning light beams. This function is useful for a parallel process for large-scale droplet manipulation. Simultaneous manipulation of a large number

of droplets can greatly save the processing time in labor-intensive diagnostics. As shown in Fig. 8, four droplets that are trapped by four laser beams are steered to rotate in opposite directions. These four laser beams are split from two laser beams by time-division scanning using two 2-D galvanometer scanning mirrors. The two droplets at the middle rotate in the counterclockwise direction, while the outer two droplets rotate in the reverse direction, without interfering with each other. This decoupled motion remains true, even when the number of the droplet becomes large due to the fully independent optical control of electrowetting electrodes.

Several device dimensions can affect droplet manipulation functions using OEW. The gap spacing of the two OEW

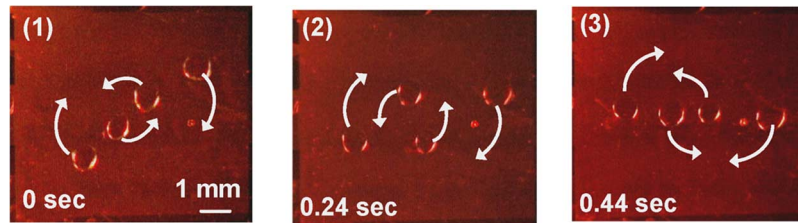


Fig. 8. Demonstration of a fully decoupled multidroplet transport function. Four droplets that are guided by four scanning laser beams are rotated in opposite directions. The two inner droplets rotate in counterclockwise direction, while the outer two droplets rotate in the clockwise direction.

surfaces is critical, particularly, for droplet injection and droplet separation functions. With a gap spacing that is too large, OEW fails to generate or separate the 1-mm-size droplet. Detail analysis of the geometry dependence of droplet functions has been provided by Cho *et al.* [11]. The smallest droplet size that can be manipulated by OEW is limited by the size of an OEW cell, which is $100\ \mu\text{m} \times 100\ \mu\text{m}$ in current devices. A smaller droplet size can be achieved by shrinking the size of OEW cells and reducing the gap spacing between two OET surfaces.

This OEW device has the potential for parallel manipulating a large array of droplets simply by increasing the active OEW area. Instead of using laser beams, a spatial light modulator such as a digital micromirror display can also be integrated to generate any arbitrary shape of optical patterns for demonstrating complex multistep droplet manipulation for parallel manipulation.

V. CONCLUSION

We have demonstrated a fully optical control droplet manipulation device using a novel OEW device. This mechanism allows light to pattern a reversible active electrowetting area in real time. We have demonstrated droplet functions including droplet injection, transportation, separation and multidroplet manipulation using light beams. This mechanism is ac frequency dependent. The optimum ac frequency for the proposed OEW device is about 100–700 Hz. The OEW mechanism does not work in the dc regime as in pure electrode base electrowetting mechanism. To manipulate a large number of droplets, the OEW surface can be extended without increasing the number of external wires. This device can potentially be driven by a spatial light modulator for processing a large droplet array in parallel to increase the throughput of droplet-based microfluidic systems.

REFERENCES

- [1] A. J. Tüds, G. A. J. Besselink, and R. B. M. Schasfoort, "Trends in miniaturized total analysis systems for point-of-care testing in clinical chemistry," *Lab Chip*, vol. 1, pp. 83–95, 2001.
- [2] C. K. Fredrickson and Z. H. Fan, "Macro-to-micro interfaces for microfluidic devices," *Lab Chip*, vol. 4, no. 6, pp. 526–533, 2004.
- [3] J. R. Millman, K. H. Bhatt, B. G. Prevo, and O. D. Velev, "Anisotropic particle synthesis in dielectrophoretically controlled microdroplet reactors," *Nat. Mater.*, vol. 4, no. 1, pp. 98–102, Jan. 2005.
- [4] P. R. C. Gascoyne, J. V. Vykoukal, J. A. Schwartz, T. J. Anderson, D. M. Vykoukal, K. W. Current, C. McConaghy, F. F. Beckera, and C. Andrews, "Dielectrophoresis-based programmable fluidic processors," *Lab Chip*, vol. 4, pp. 299–309, 2004.
- [5] A. R. Wheeler, H. Moon, C. A. Bird, R. O. Loo, C. J. Kim, J. A. Loo, and R. L. Garrell, "Digital microfluidics with in-line sample purification for proteomics analyses with MALDI-MS," *Anal. Chem.*, vol. 77, no. 2, pp. 534–540, 2005.

- [6] O. D. Velev, B. G. Prevo, and K. H. Bhatt, "On-chip manipulation of free droplets," *Nature*, vol. 426, no. 6966, pp. 515–516, Dec. 2003.
- [7] J. A. Schwartz, J. V. Vykoukal, and P. R. C. Gascoyne, "Droplet-based chemistry on a programmable micro-chip," *Lab Chip*, vol. 4, no. 1, pp. 11–17, Feb. 2004.
- [8] M. Vallet, B. Berge, and L. Vovelle, "Electrowetting of water and aqueous solutions on poly(ethylene terephthalate) insulating films," *Polymer*, vol. 37, no. 12, pp. 2465–2470, 1996.
- [9] M. G. Pollack, R. B. Fair, and A. D. Shenderov, "Electrowetting-based actuation of liquid droplets for microfluidic applications," *Appl. Phys. Lett.*, vol. 77, no. 11, pp. 1725–1726, Sep. 2000.
- [10] J. Lee, H. Moon, J. Fowler, T. Schoellhammer, and C. J. Kim, "Electrowetting and electrowetting-on-dielectric for microscale liquid handling," *Sens. Actuators A, Phys.*, vol. 95, no. 2, pp. 259–268, Jan. 2002.
- [11] S. K. Cho, H. J. Moon, and C. J. Kim, "Creating, transporting, cutting, and merging liquid droplets by electrowetting-based actuation for digital microfluidic circuits," *J. Microelectromech. Syst.*, vol. 12, no. 1, pp. 70–80, 2003.
- [12] J. Fowler, H. Moon, and C. J. Kim, "Enhancement of mixing by droplet-based microfluidics," in *Proc. 15th IEEE Int. Conf. Micro Electro Mech. Syst.*, 2004, pp. 97–100.
- [13] A. R. Wheeler, H. Moon, C. J. Kim, J. A. Loo, and R. L. Garrell, "Electrowetting-based microfluidics for analysis of peptides and proteins by matrix-assisted laser desorption/ionization mass spectrometry," *Anal. Chem.*, vol. 76, no. 16, pp. 4833–4838, 2004.
- [14] V. Srinivasan, V. K. Pamula, and R. B. Fair, "Droplet-based microfluidic lab-on-a-chip for glucose detection," *Anal. Chim. Acta*, vol. 507, no. 1, pp. 145–150, Apr. 2004.
- [15] J. Gong, S. K. Fan, and C. J. Kim, "Portable digital microfluidics platform with active but disposable Lab-On-Chip," in *Proc. 17th IEEE Int. Conf. Micro Electro Mech. Syst.*, 2004, pp. 355–358.
- [16] S. K. Fan, C. Hashi, and C. J. Kim, "Manipulation of multiple droplets on $N \times M$ grid by cross-reference EWOD driving scheme and pressure-contact packaging," in *Proc. 16th IEEE Annu. Int. Conf. Micro Electro Mech. Syst.*, 2003, pp. 694–697.
- [17] P. Y. Chiou, H. Moon, H. Toshiyoshi, C. J. Kim, and M. C. Wu, "Light actuation of liquid by optoelectrowetting," *Sens. Actuators A, Phys.*, vol. 104, no. 3, pp. 222–228, May 2003.



Pei-Yu Chiou (M'06) received the B.S. degree in mechanical engineering from National Taiwan University, Taipei, Taiwan, R.O.C., the M.S. degree in electrical engineering from the University of California, Los Angeles (UCLA), and the Ph.D. degree in electrical engineering and computer sciences from the University of California, Berkeley (UC Berkeley), in 2005.

He joined the faculty of UCLA as a member of the Department of Mechanical and Aerospace Engineering in 2006, after postdoctoral work at UC Berkeley.

His research interests are bioMEMS and biophotonics.

Zehao Chang received the M.S. degree in electrical engineering and the M.F.A. degree in design/media arts in 2002 and 2005, respectively, from the University of California, Los Angeles (UCLA), where he conducted research in applying optoelectric wetting principles to MEMS devices.

He is currently with UCLA, working on design and graphics programming, with emphasis on interactive installations.



Ming C. Wu (S'82–M'83–SM'00–F'02) received the B.S. degree in electrical engineering from National Taiwan University, Taipei, Taiwan, R.O.C., and the M.S. and Ph.D. degrees in electrical engineering and computer sciences from the University of California, Berkeley, in 1985 and 1988, respectively.

From 1988 to 1992, he was a member of Technical Staff with AT&T Bell Laboratories, Murray Hill, NJ. From 1992 to 2004, he was a Professor with the Department of Electrical Engineering, University of California, Los Angeles, where he also served as the Vice Chair for the Industrial Affiliate Program and the Director of the Nanoelectronics Research Facility. In 2004, he moved to the University of California, Berkeley, where he is currently a Professor of electrical engineering and computer sciences. He is also a Codirector of the Berkeley Sensor and Actuator Center. He is the author or coauthor of six book chapters, more than 135 journal papers, and 280 papers published in conference proceedings. He is the holder of 14 U.S. patents. His research interests include optical microelectromechanical systems, high-speed semiconductor optoelectronics, nanophotonics, and biophotonics.

Prof. Wu is a member of the Optical Society of America. He was a Packard Foundation Fellow from 1992 to 1997. He is the founding Co-Chair of the IEEE/LEOS Summer Topical Meeting on Optical MEMS (1996) and the predecessor of the IEEE/LEOS International Conference on Optical MEMS. He has served on the program committees of many technical conferences, including the International Conference on Microelectromechanical Systems, Optical Fiber Communication Conference, Conference on Lasers and Electro-Optics, Lasers and Electro-Optics Society Annual Meeting, Microwave Photonics Conference, International Electron Devices Meeting, Device Research Conference, and International Solid-State Circuit Conference. He has also served as a Guest Editor of two special issues of IEEE journals on Optical MEMS.